# Analysis of CV-QKD Coexistence with Counter-Propagating C-Band Dense WDM Channels

Wasim Ahamed*[†‡], Utku Akin[†§], Jonas Berl[†¶], Mario Wenning[†§], Chigo Okonkwo[‡], Tobias Fehenberger[†]
[†]*Adva Network Security, Germany* [‡]*High-Capacity Optical Transmission Lab, TU/e, Netherlands*
[§]*Institute for Communications Engineering, TUM, Germany* [¶]*Communications Engineering Lab, KIT, Germany*
**SkWasim.Ahamed@advasecurity.com*

***Abstract*—The coexistence of quantum and dense wavelength-division multiplexed (DWDM) channels offers a practical route for integrating continuous-variable quantum key distribution (CV-QKD) into deployed fiber networks. In this paper, we employ numerical simulations to investigate the impact of classical channel placement on CV-QKD system performance in a counter-propagating configuration, accounting for fiber nonlinearities and spontaneous Raman scattering (SpRS). We demonstrate that, as a consequence of the wavelength-dependent behavior of SpRS, smaller guard bands between the classical and quantum channels can be preferable to maximizing the spectral separation.**

## I. Introduction

In recent years, quantum computing has seen remarkable advances, raising critical concerns about long-term data security. Continuous-variable quantum key distribution (CV-QKD) provides a quantum-safe alternative to classical key exchange mechanisms, offering information-theoretic security based on fundamental quantum principles. Its compatibility with commercial off-the-shelf telecommunication components makes CV-QKD a promising candidate for the integration into optical networks [1], [2].

To enable cost-efficient integration into optical networks, quantum signals are preferably co-transmitted with classical dense wavelength-division multiplexing (DWDM) data channels over a shared optical fiber. The scenario in which both signals propagate in the same direction is referred to as co-propagating, while propagation in opposite directions defines the counter-propagating case. Due to fiber nonlinearities and spontaneous Raman scattering (SpRS), the coexistence of DWDM channels and the quantum channel introduces excess noise, which can significantly impair the performance of CV-QKD in the absence of adequate mitigation [3]–[5]. While multiple experiments have demonstrated the practical feasibility of co-existence of CV-QKD with DWDM classical traffic over metropolitan and long-haul fiber networks [6]–[8] and several models for SpRS in the co- and counter-propagating scenario exist [3], [9], a comprehensive simulation framework that includes both effects from fiber nonlinearity and SpRS for counter-propagation is still lacking.

In this work, we develop a simulation methodology for the counter-propagation scenario and study the impact of classical channel placement on the quantum channel in terms of excess noise. Our results reveal the counterintuitive finding that a smaller spectral separation between the DWDM channels and the quantum channel can be advantageous, highlighting the need for strategic wavelength planning rather than guard-band intuition alone.

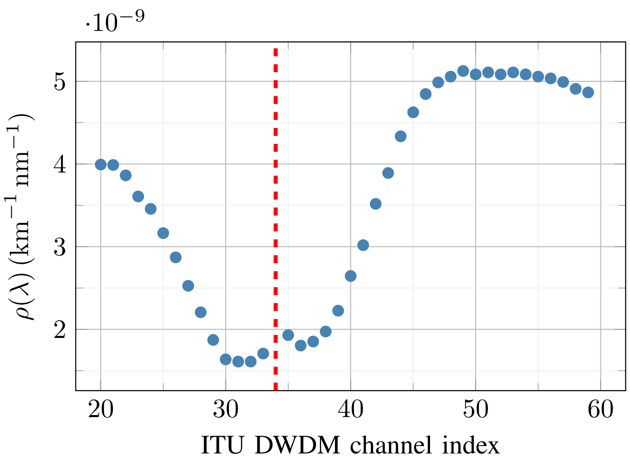


Fig. 1. Raman cross-section into ITU channel C34 for different ITU DWDM channels.

## II. Simulation Framework

Inspired by the numerical methods for distributed Raman amplifiers in long-haul communication [10] and the generalized nonlinear Schrödinger equation [11], we have modified the conventional numerical split-step Fourier method (SSFM) and extended it for the counter-propagation case. Given the computational cost, we have chosen $2^{14}$ symbols for the simulation without using a fixed seed. We have seen that this is sufficient to capture statistical trends in parameter estimation by evaluating signal-to-noise ratio and transmittance at each step of SSFM and comparing it with the expected values.

### *A. Assumptions*

Due to the relatively low power of the CV-QKD signal, its nonlinear impact on the classical DWDM channels is negligible. We therefore implement a two-step modified SSFM that is sufficient to capture the impairments imposed by the classical channels on the CV-QKD signal. First, the propagation of classical data channels was simulated using the standard SSFM approach, and the power spectral density (PSD) was stored at each step over the entire simulation window. Later, the quantum channel's propagation was simulated in the opposite

978-3-903176-78-2 © 2026 IFIP

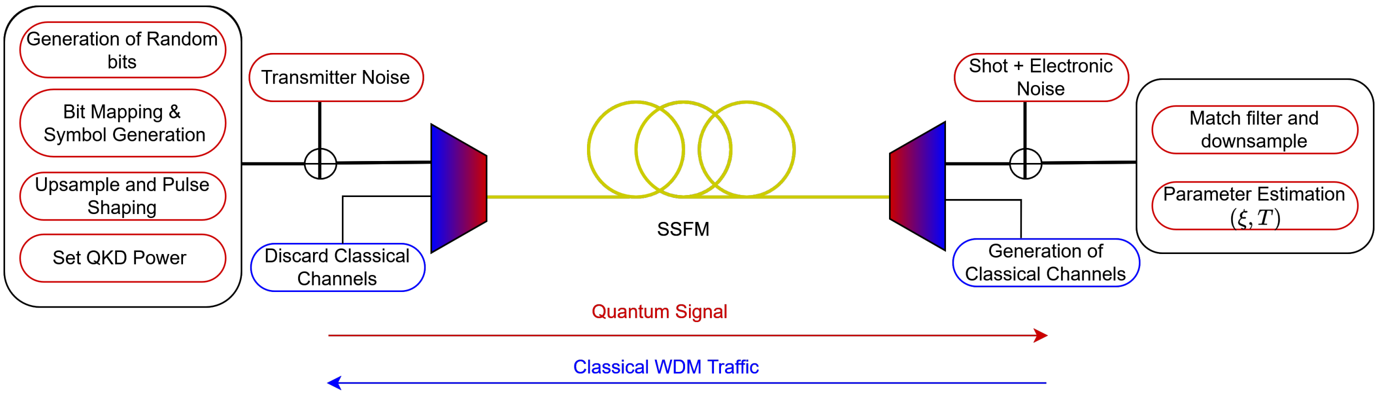


Fig. 2. Schematic of the simulation setup. Red and blue colors highlight the quantum and classical signal paths, including their respective propagation and DSP chains.

direction, using the stored PSDs to calculate the nonlinear contribution assuming a fiber nonlinear coefficient of $\gamma = 1.3\ \mathrm{W}^{-1}\ \mathrm{km}^{-1}$.

Figure 1 shows the Raman cross-section, $\rho(\lambda)$, into ITU channel C34, evaluated for different $100\,\mathrm{GHz}$-spaced ITU DWDM channels (C34 indicated by the red vertical line). The values of $\rho(\lambda)$ for C34 are obtained by extracting experimental data from [12]. Additionally, the assumptions from Refs. [13], [14] were adopted to approximately calculate $\rho(\lambda)$ due to remaining channels. These channel-dependent $\rho(\lambda)$ values are then used at each SSFM step to synthesize a band-limited complex noise sequence representing SpRS, thereby preserving its stochastic nature throughout the propagation.

### *B. Simulation Setup and Parameters*

Figure 2 illustrates the simulation setup used to analyze the coexistence of a CV-QKD signal multiplexed in wavelength with counter-propagating classical channels in a standard single mode fiber. At the CV-QKD transmitter (left side of the figure), quantum states are generated by mapping random bits onto $256$-QAM symbols at a rate of $150\,\mathrm{Mbd}$. The symbol sequence is then upsampled, by a factor chosen to meet the required simulation bandwidth, and pulse-shaped with a root-raised-cosine (RRC) filter. The launch power is set to $6.2\,\mathrm{SNU}$ to achieve a quantum-level signal, and to reflect practical preparation noise, a transmitter noise modeled as a zero-mean white Gaussian noise (WGN) with variance $0.03\,\mathrm{SNU}$ is added. The quantum signal is then wavelength-multiplexed with classical channels that are generated at the fiber end with respect to the CV-QKD signal with a launch power of $0\,\mathrm{dBm}$ per channel. Fiber propagation is simulated using the proposed SSFM method, after which the QKD signal is demultiplexed from the classical traffic.

At the CV-QKD receiver, shot noise and electronic noise are included as zero-mean additive WGN with variances of $1\,\mathrm{SNU}$ and $0.1\,\mathrm{SNU}$, respectively. Out-of-band noise is suppressed using a matched RRC filter, and the noisy quantum states are obtained through downsampling. Finally, parameter estimation is performed to quantify transmittance and excess noise which includes the residual noise on the quantum states other than receiver noise. The results in the following section show that the excess noise is primarily driven by preparation noise, SpRS and nonlinear inter-channel crosstalk.

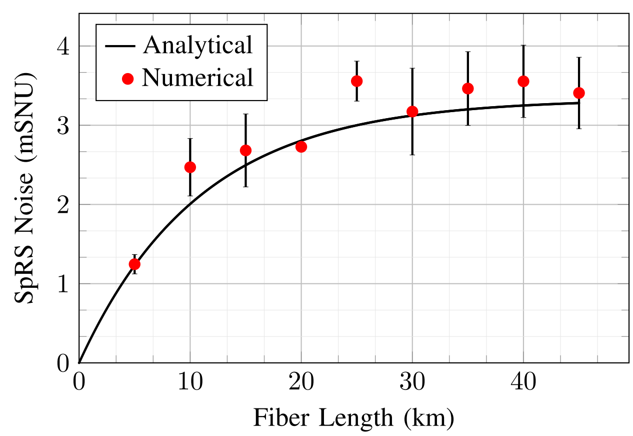


Fig. 3. Comparison between numerically simulated SpRS noise and the theoretical prediction. Error bars indicate statistical variation across three independent runs.

## III. Simulation Results

To validate our simulation framework, we quantify the SpRS noise as a function of fiber length and compare the results with the analytical approach in [3]. Therefore, we assume the quantum channel as ITU C58 and one classical channel as ITU C34, respectively. Figure 3 shows the resulting SpRS noise based on the analytical model and the simulation framework. For the numerical results, we run three independent simulations for each distance.

The results show that the numerical simulations agree with the analytical values at the measurement points, validating our simulation framework. In addition, Fig. 3 shows that the SpRS noise increases with distance due to counter-propagation. Lastly, we see fluctuations in the numerical results as a

TABLE I
CONFIGURATION OVERVIEW

| Configuration | Quantum | Classical |
|---|---|---|
| A | C34 | None |
| B | C34 | C33, C35 |
| C | C34 | C21, C47 |

consequence of random seeds in the simulation and estimation errors due to the limited number of symbols.

After verifying the simulation framework, we analyze different settings of classical and quantum channels. Hence, we quantify the excess noise depending on the distance for configurations A, B, and C as summarized in Tab. I.

Figure 4 depicts the numerical results for the excess noise depending on the fiber length and the three configurations A, B, and C. For each distance, we perform five simulation runs and depict the mean values with error bars. For all configurations, Fig. 4 shows decreasing excess noise with increasing distance. All configurations start around $30\,\mathrm{mSNU}$ due to the excess noise from the transmitter and are subject to attenuation, leading to an approximately exponential decay over distance for configuration A. Moreover, adding classical channels (configurations B and C) increases excess noise. We differentiate the nonlinear effects from classical channels into cross-phase modulation (XPM) and SpRS. The classical channels in configuration B have a smaller spectral separation to the quantum channel compared to configuration C. Consequently, the XPM for configuration B is higher compared to C. Since the excess noise for configuration C is larger compared to configuration B, Fig. 4 shows that SpRS is the dominant effect compared to the XPM. The Raman cross-section corresponding to configurations B and C are $3.64 \times 10^{-9}\,\mathrm{km}^{-1}\mathrm{nm}^{-1}$ and $8.97 \times 10^{-9}\,\mathrm{km}^{-1}\mathrm{nm}^{-1}$, respectively. This difference makes the excess noise in configuration C higher than in configuration B, although the guard band between the quantum and classical channels is larger for configuration C. The study in [3] shows comparable findings. Based on the results in Fig. 4, we recommend configuration B compared to C. Similar to the previous results, the figure depicts comparable fluctuation due to different random seeds and estimation errors.

## IV. CONCLUSION

We investigated the impact of classical data traffic on counter-propagating quantum signals by comparing different WDM channel configurations. The numerical simulation results, based on a modified SSFM, indicate that SpRS is the dominant contributor to excess noise, severely impacting the performance of CV-QKD. Due to the wavelength-dependence of SpRS, we show that WDM channel configurations with larger spectral separation to the quantum channel may perform worse than closer spaced channels. Rather than relying solely on guard-band intuition, these results provide guidance for optimizing spectrum assignment in QKD-secured optical networks.

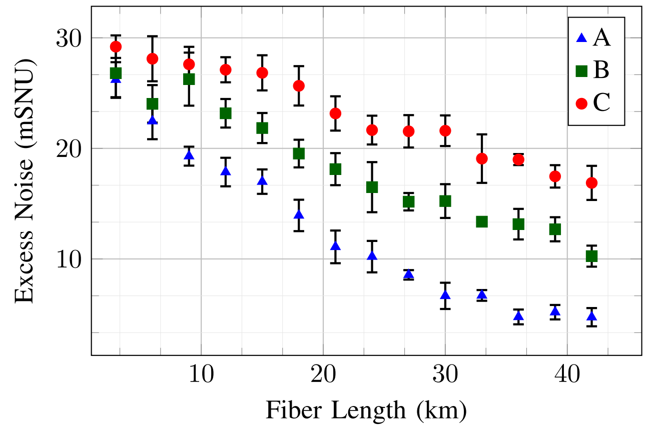


Fig. 4. Evolution of excess noise over the fiber length for different configurations. Statistical variation due to 5 times runs.


## ACKNOWLEDGMENTS

This work is partially funded by the European Union under the project QuNEST (Grant Agreement: 101120422). Views and opinions expressed are, however, those of the author(s) only and do not necessarily reflect those of the European Union or REA. Neither the European Union nor the granting authority can be held responsible for them.

This work is partially funded by the German Federal Ministry of Research, Technology and Space under the project SEQUIN (Grant ID 16KIS2132K).


## REFERENCES


[1] F. Grosshans *et al.*, “Continuous variable quantum cryptography using coherent states,” *Physical Review Letters*, vol. 88, no. 5, 057902, 2002.

[2] C. Weedbrook *et al.*, “Gaussian quantum information,” *Reviews of Modern Physics*, vol. 84, pp. 621–669, 2012.

[3] R. Kumar *et al.*, “Coexistence of continuous-variable QKD with intense DWDM classical channels,” *New Journal of Physics*, vol. 17, 2015.

[4] P. Jouguet *et al.*, “Experimental demonstration of long-distance continuous-variable quantum key distribution,” *Nature Photonics*, vol. 7, pp. 378–381, 2013.

[5] N A Peters *et al.*, “Dense Wavelength Multiplexing of 1550 nm QKD with Strong Classical Channels in Reconfigurable Networking Environments,” *New Journal of Physics Article*, December 2008.

[6] Adnan A.E. Hajomer *et al.*, “Coexistence of continuous-variable quantum key distribution and classical data over 120 km fiber,” *Physical Review Letters*, vol. 132, 020802, 2024.

[7] Tobias A. Eriksson *et al.*, “Wavelength Division Multiplexing of 194 Continuous Variable Quantum Key Distribution Channels,” *Journal of Lightwave Technology*, vol. 38, no. 8, April 2020.

[8] F. Kiselev *et al.* “Performance of subcarrier-wave quantum key distribution in the presence of spontaneous Raman scattering noise generated by classical DWDM channels,” *J. Opt. Soc. Amer. B*, Opt. Phys., vol. 38, no. 2, pp. 595–601, 2021.

[9] Flóra Viktória Kárpát *et al.*, “Investigation of Nonlinear Raman Scattering in Optical Quantum Communication Systems,” *IET Quantum Communication*, vol.6, no.1, 2025.

[10] Yao Xie *et al.*, “A Channel Model to Deal with Distributed Noises and Nonlinear Effects in a Fiber System with Distributed Raman Amplifiers,” vol. 10, no. 1, Art. no. 133, 2019.

[11] G. P. Agrawal, “Stimulated Raman scattering,” in “Nonlinear Fiber Optics”, 5th ed. Oxford, U.K.: *Elsevier*, 2013, ch. 8.

[12] P. Eraerds *et al.*, “Quantum key distribution and 1 Gbps data encryption over a single fibre,” *New Journal of Physics*, vol. 12, no. 6, 2010.

[13] Masab Iqbal *et al.*, “SDN-enabled CV-QKD and classical channels coexistence: key insights for DWDM,” *Journal of Optical Communications and Networking*, Vol. 17, No. 6, June 2025.

[14] Rui Lin *et al.*, “Modeling and minimizing spontaneous Raman scattering for QKD secured DWDM networks,” *IEEE Communications Letters*, vol. 25, no. 12, pp. 3918-3921, 2021.